Dynamics of lattice vibrations for one-dimensional commensurate and incommensurate composites with harmonic interaction

1997 J. Phys. A: Math. Gen. 30 4199

(http://iopscience.iop.org/0305-4470/30/12/011)

J. Phys. A: Math. Gen. **30** (1997) 4199–4214. Printed in the UK PII: S0305-4470(97)81482-5

Dynamics of lattice vibrations for one-dimensional commensurate and incommensurate composites with harmonic interaction

O Radulescu and T Janssen

Katholieke Universiteit Nijmegen, Theoretische Fysica, Postbus 9010, 6500 GL Nijmegen, the Netherlands

Received 30 January 1997

Abstract. We introduce a model that generalizes the Frenkel–Kontorova model and describes a one-dimensional (1D) composite system made of two subsystems which are treated on an equal footing. The gap structure of the phonon energy spectrum and the character of lattice vibration are studied. We show that the phason mode may be pinned or not depending on the form of the intersubsystem potential. For a weak intersubsystem interaction the structure of the phonon energy spectrum is universal and may be revealed by a gnomonic projection of $\mathbb{Z}^3$ onto the plane. For a short-range harmonic interaction there are similarities between this model of composite and 1D quasicrystals.

1. Introduction

The acceptance of the name 'composite' in materials science is large, applying to materials whose structure contains at least two different subsystems. The results of this paper apply to composite systems containing crystalline subsystems which differ by the period along one or several crystalline directions. In this sense the name 'composite' applies to misfit layer, chimney-ladder, intergrowth, and Vernier structures (see Yamamoto 1993 for a comprehensive presentation). The crystallographic structure of these compounds has been extensively investigated and sometimes requires a four-dimensional (4D) or five-dimensional (5D) superspace description, as the number of rationally independent periods is greater than 3.

The ratio of the periods of the two subsystems along different directions in a composite may be rational or irrational. We speak then of commensurate and incommensurate composites, respectively. The incommensurate composites belong to the larger class of incommensurate crystals. The incommensurability of the composites comes neither from the modulation of a basic three-dimensional (3D) crystalline structure (as for the modulated incommensurate crystals) nor from the quasiperiodic repetition of some structural units (as for the quasicrystals and polytypes), but from the existence of several interpenetrating, mutually incommensurate crystalline structures.

The long wavelength lattice dynamics of composites has been studied in the continuous approximation by Emery and Axe (1978), Axe and Bak (1982), Finger and Rice (1983) for the intergrowth compound $Hg_{3-\delta}AsF_6$. Semidiscrete models of composites have been proposed by Theodorou and Rice (1978) and Ishii (1983). In these models the treatment of the intersubsystems interaction term does not fully emphasize the discreteness effects.

0305-4470/97/124199+16$19.50

Recently interest in composites has grown. In many of these compounds there is no clear host lattice, and one has to treat the subsystems on an equal footing. Then the picture of a (rigid or deformable) substrate is no longer valid.

We propose here a rigorous model of a discrete one-dimensional-(1D) composite, composed of two flexible atomic chains with different natural periods. This model has two subsystems which play the same role. The main problem is that of the character of the lattice vibrations and the gap structure in such a symmetric case. The incommensurate structure is obtained as the limit of commensurate structures with increasing period. The intrachain and interchain interaction is considered to be described as a sum of pair potentials. The general model is introduced in section 2. In section 3 we consider the interchain interaction to be harmonic and short range in order to compute the phonon spectrum of the double chain. The problem discussed here is the gap structure of the spectrum. For the first time the hierarchical nature of the gap structure is shown in the case of a double chain, extending previous results that are valid for simple Frenkel–Kontorova chains. Section 4 discusses the possibility of the existence of a sliding mode and proposes analytical expressions for the speed of sound.

2. General settings for the dynamics of a double chain with pair potential interaction in the harmonic approximation

Let $x_n^{(1)}$ and $x_m^{(2)}$ be the positions of the atoms on the first chain and on the second chain, respectively. Let us suppose that the potential energy of the double chain, is a sum of pair potentials

$$\mathcal{V}(\{x_n^{(1)}; x_m^{(2)}\}) = \sum_{n<n'} \mathcal{V}_{n,n'}^{(1,1)}(x_n^{(1)} - x_{n'}^{(1)}) + \sum_{m<m'} \mathcal{V}_{m,m'}^{(2,2)}(x_m^{(2)} - x_{m'}^{(2)}) + \sum \mathcal{V}_{n,m}^{(1,2)}(x_n^{(1)} - x_m^{(2)}). \tag{1}$$

In the harmonic approximation, and supposing that inside each chain only first-neighbour atoms interact, the above expression becomes:

$$\mathcal{V}(\{u_n^{(1)}; u_m^{(2)}\}) = \frac{k^{(1)}}{2} \sum [u_n^{(1)} - u_{n-1}^{(1)}]^2 + \frac{k^{(2)}}{2} \sum [u_m^{(2)} - u_{m-1}^{(2)}]^2 + \sum_{(n,m)\in\mathcal{B}} \frac{k_{n,m}^{(1,2)}}{2} [u_n^{(1)} - u_m^{(2)}]^2 \tag{2}$$

where $u_n^{(1)}$ and $u_m^{(2)}$ are the displacements of the atoms with respect to their static equilibrium positions, and the elastic constants are second derivatives of the pair potentials calculated at distances between atoms at static equilibrium.

Set $\mathcal{B}$ contains the set of pairs of indices of atoms in interaction (interchain bonds).

If the masses of the atoms on the two chains are $m_i, i = 1, 2$, then the vibration frequencies are the square roots of the eigenvalues of the force operator $\boldsymbol{F}$:

$$\boldsymbol{F} = \boldsymbol{F}_0 + \boldsymbol{F}' \tag{3}$$

where, using reduced coordinates $y_n^{(i)} = \sqrt{m_i} u_n^{(i)}$,

$$\boldsymbol{F}_0(y_n^{(1)}, y_m^{(2)}) := (\omega_1^2[2y_n^{(1)} - y_{n+1}^{(1)} - y_{n-1}^{(1)}], \omega_2^2[2y_m^{(2)} - y_{m+1}^{(2)} - y_{m-1}^{(2)}]) \tag{4}$$

$$\boldsymbol{F}'(y_n^{(1)}, y_m^{(2)}) := \left(\frac{1}{m_1} \left(\sum_{r\in\mathcal{B}_n} k_{n,r}^{(1,2)} \right) y_n^{(1)} - \frac{1}{\sqrt{m_1 m_2}} \sum_{r\in\mathcal{B}_n} k_{n,r}^{(1,2)} y_r^{(2)}, \frac{1}{m_2} \left(\sum_{s\in\mathcal{B}^m} k_{s,m}^{(1,2)} \right) y_m^{(2)} - \frac{1}{\sqrt{m_1 m_2}} \sum_{s\in\mathcal{B}^m} k_{s,m}^{(1,2)} y_s^{(1)} \right) \tag{5}$$

with $\mathcal{B}_n := \{r|(n,r) \in \mathcal{B}\}$ and $\mathcal{B}^m := \{s|(s,m) \in \mathcal{B}\}$, $\omega_i^2 := \frac{k^{(i)}}{m_i}$, $i = 1, 2$.

The harmonic composite is called (p, q) periodic if $\mathcal{B} = (p, q) + \mathcal{B}$, $k^{(1,2)}_{n+p,m+q} = k^{(1,2)}_{n,m}$. In this case,

$$\begin{aligned} \mathcal{B}_{n+p} &= \mathcal{B}_n + q \\ \mathcal{B}^{m+q} &= \mathcal{B}_m + p \\ \mathcal{B} &= \bigcup_{n\in\mathbb{Z}} \{\mathcal{B}_0^{p,q} + (np, nq)\} \end{aligned} \tag{6}$$

where $\mathcal{B}_0^{p,q}$ is the primitive unit cell of the (p, q) periodic set $\mathcal{B}$.

Let $T_{p,q}$ be the (p, q) translation operator:

$$T_{p,q}(y_n^{(1)}, y_m^{(2)}) := (y_{n+p}^{(1)}, y_{m+q}^{(2)}). \tag{7}$$

For a (p, q) periodic composite, the (p, q) translation operator commutes with the force operator:

$$[T_{p,q}, \boldsymbol{F}] = 0. \tag{8}$$

Therefore, the eigenvalue problem for the infinite-dimensional operator $\boldsymbol{F}$ is reduced using Bloch theory (van Mouche 1988) to the eigenvalue problem for a family of $(p + q)$-dimensional operators (dynamic matrix) $\mathbf{F}_\theta^{p,q} := \boldsymbol{F}|\,\mathrm{Ker}(T_{p,q} - \mathrm{e}^{\mathrm{i}\theta}\,\mathrm{Id})$, the values of θ being restricted to the Brillouin zone $\theta \in (-\pi, \pi]$. Precisely, one has:

$$\mathrm{Spec}(\boldsymbol{F}) = \bigcup_{\theta\in(-\pi,\pi]} \mathrm{Spec}\,\mathbf{F}_\theta^{p,q}. \tag{9}$$

The same reduction applied to $\boldsymbol{F}_0$ and $\boldsymbol{F}'$ yields $\mathbf{F}_\theta^{p,q} = \mathbf{F}_{p,q}^0(\theta) + \mathbf{F}'_{p,q}(\theta)$

$$\mathbf{F}_{p,q}^0(\theta) = \left[\begin{array}{c|c} \omega_1^2\mathbf{D}_p & \mathbb{O} \\ \hline \mathbb{O} & \omega_2^2\mathbf{D}_q \end{array}\right] \tag{10}$$

where $\mathbf{D}_p$ is the dynamical matrix of a single harmonic chain in p-periodic folded zone representation

$$\mathbf{D}_p = \begin{bmatrix} 2 & -1 & 0 & \overset{p}{\ldots} & 0 & -\mathrm{e}^{-\mathrm{i}\theta} \\ -1 & 2 & -1 & \ldots & 0 & 0 \\ \vdots & & & & & \vdots \\ -\mathrm{e}^{\mathrm{i}\theta} & 0 & 0 & \ldots & -1 & 2 \end{bmatrix} \tag{11}$$

where $\mathbf{F}_{p,q}^0(\theta)$ is the dynamical matrix of the double chain without interchain interaction. It has p eigenvectors representing waves propagating in the first chain and q eigenvectors representing waves propagating in the second chain.

In a suitably chosen basis, the above eigenvectors read:

$$\begin{aligned} v_k^{(1)}(\theta) &= \frac{1}{\sqrt{p}}(1, z_k, z_k^2, \ldots, z_k^{p-1}, 0, \ldots, 0) \\ z_k &= \exp\left[\frac{\mathrm{i}}{p}(\theta + 2\pi k)\right] \qquad k = 0, \ldots, p-1 \\ v_l^{(2)}(\theta) &= \frac{1}{\sqrt{q}}(0, \ldots, 0, 1, w_l, w_l^2, \ldots, w_l^{q-1}) \\ w_l &= \exp\left[\frac{\mathrm{i}}{q}(\theta + 2\pi l)\right] \qquad l = 0, \ldots, q-1 \end{aligned} \tag{12}$$

and the corresponding eigenvalues are:

$$\lambda_k^{(1)}(\theta) = 4\omega_1^2 \sin^2 \frac{1}{2}\frac{\theta + 2\pi k}{p}$$
$$\lambda_l^{(2)}(\theta) = 4\omega_2^2 \sin^2 \frac{1}{2}\frac{\theta + 2\pi l}{q}. \tag{13}$$

For some values of k, l, θ, some of the above eigenvalues become doubly degenerate. One has four situations:

(1) intercrossing (double-chain modes), which is

$$\lambda_k^{(1)}(\theta) = \lambda_l^{(2)}(\theta) \tag{14}$$

for θ inside the Brillouin zone, $0 < |\theta| < \pi$.

(2) Acoustic degeneracy, coming from the translation symmetry of both chains:

$$\lambda_0^{(1)}(0) = \lambda_0^{(2)}(0) = 0. \tag{15}$$

(3) Centre of zone degeneracy (in single-chain modes):

$$\lambda_k^{(1)}(0) = \lambda_{k'}^{(1)}(0) \qquad \text{or} \qquad \lambda_l^{(2)}(0) = \lambda_{l'}^{(2)}(0). \tag{16}$$

(4) Border of zone degeneracy (in single-chain modes only):

$$\lambda_k^{(1)}(\pm\pi) = \lambda_{k'}^{(1)}(\pm\pi) \qquad \text{or} \qquad \lambda_l^{(2)}(\pm\pi) = \lambda_{l'}^{(2)}(\pm\pi). \tag{17}$$

The introduction of the interaction term $\mathbf{F}'_{p,q}(\theta)$ raises the degeneracy and produces gaps in the spectrum of $\boldsymbol{F}$. The situation is more complex for a double chain than it is in the case of a simple chain under a periodic perturbation (de Lange and Janssen 1981), because of the intercrossing. For a simple chain any degeneracy is of the type (3) or (4), and any degeneracy raise produces a gap. It is not the case of the double chain, where, for small perturbations, gaps appear only at the intercrossing, and only if the derivatives $\mathrm{d}\lambda_k^{(1)}(\theta)/\mathrm{d}\theta$ and $\mathrm{d}\lambda_l^{(2)}(\theta)/\mathrm{d}\theta$ have opposite signs (see figure 1). Raising the degeneracy in situations (2)–(4) produces only a van Hove singularity edge in the density of states. For low values of the coupling constant $k^{(1,2)}$, modes between two such singularity edges are waves propagating in only one chain, and being extinct in the other chain. Let us call the region between two singularity edges 'single gap'. Modes propagating in the second chain are pushed out of the single gap by the interchain interaction, and therefore the density of states is about two times lower inside than outside the single gap. For larger values of the coupling constant, nonlinear effects destroy this simple image. Let us define a relative participation ratio as follows

$$l^{(2)} := \frac{p}{q}\frac{\sum_{i=1}^{q}(u_i^{(2)})^2}{\sum_{i=1}^{p}(u_i^{(1)})^2}. \tag{18}$$

In figure 1(c) we represent the contribution to the density of states of modes for which the relative participation ratio $l^{(2)}$ of atoms in the second chain is greater than 0.1. For small $k^{(1,2)}$ the atoms of the second chain do not participate to modes inside single gaps of this chain.

Both true (double) gap edges and single gap edges are analytic functions of the interaction parameter $k^{(1,2)}$. It may happen that for high values of $k^{(1,2)}$, a single gap of one chain superpose to a single gap of the second chain and a true (double) gap (containing no modes) arises.

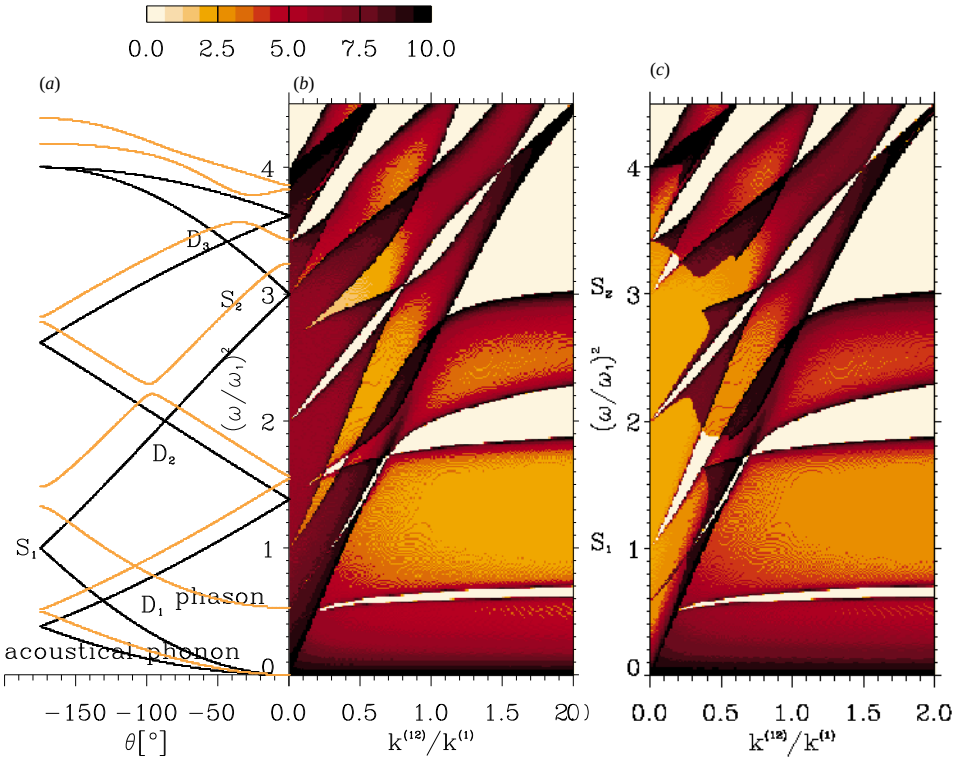

Figure 1. (*a*) Folded phonon branches of a (5, 3) periodic composite before and after switching on the interchain interaction; true gaps open at the intercrossings D_1, D_2, D_3, and single gaps of the second chain open at S_1, S_2. (*b*) Density of states as a function of $k^{(1,2)}/k^{(1)}$ for a (5, 3) periodic composite. DOS is per atom and for an energy unit $4\omega_1^2$. (*c*) Density of states with relative participation ratio $l^{(2)} \geqslant 0.1$; notice that there are no such states inside single gaps at S_1, S_2. The results presented here were obtained numerically, using LINPACK procedures. We have chosen $m_1 = m_2$ and $k^{(1)} = k^{(2)}$.

(This figure can be viewed in colour in the electronic version of the article; see `http://www.iop.org/EJ/welcome`)

3. The short-range, harmonic interaction composite

3.1. Presentation of the model

Let us illustrate the above general remarks, for sets $\mathcal{B}_0^{p,q}$ (primitive unit cell of $\mathcal{B}$) of pairs of interacting atoms defined as follows

$$\begin{aligned} \mathcal{B}_0^{p_1+p_2,q_1+q_2} &= \mathcal{B}_0^{p_1,q_1} \bigcup \{(p_1,q_1) + \mathcal{B}_0^{p_2,q_2}\} \\ \mathcal{B}_0^{1,1} &= \{(1,1)\} \\ \mathcal{B}_0^{2,1} &= \{(1,1),(2,1)\} \end{aligned} \tag{19}$$

where it is supposed that $p_1/q_1 < p_2/q_2$. Starting with the (1, 1) and (2, 1) periodic composites, one may iterate (19) and obtain all intermediate periodic structures ((p, q) periodic composites such that $1 \leqslant p/q \leqslant 2$). The set of rational numbers p/q increases at each step of the construction as follows. Between successive rational numbers $p_1/q_1 \leqslant p_2/q_2$ which are available at step n, an intermediate rational number is introduced

at step $n+1(\frac{p_1}{q_1} \leqslant \frac{p_1+p_2}{q_1+q_2} \leqslant \frac{p_2}{q_2})$. The above recursion is the well known mediant construction and at the nth step one gets the Farey series of order n (see Hua 1982) translated by 1. In order to extend the construction from the interval $[1, 2]$ to all positive rational numbers, one has to define $\mathcal{B}_0^{p,1}$ for $p \in \mathbb{N}$, and then apply (19) inside each interval $[p, p+1]$.

Let us also consider that the interchain elastic constants are all the same ($k_{n,m}^{(1,2)} = k^{(1,2)}$).

The physical significance of the above choice of sets $\mathcal{B}_0^{p,q}$ is as follows. Interchain interaction is considered to be short range, each atom on the chain of lower period (let us consider it to be chain 1, and consequently $p > q$) interacts with only one atom on the other chain (chain 2), the one which is closest to it (thus $\sharp\mathcal{B}_n = 1$). In the case of equal distances, the leftmost atom is chosen. This particular choice of interchain interaction coincides with the one used by Aubry (1982) for the exactly soluble model of a harmonic chain on a non-deformable substrate with parabolic potential. Here we replace the substrate by a deformable second chain.

This short-range, harmonic interaction composite is in many ways similar to a quasicrystal. First, notice that harmonicity of the interaction implies that the force operator depends only on the connectivity of the atoms (set $\mathcal{B}$). We suppose that the set $\mathcal{B}$ does not change when the interchain interaction is switched on. The flexible chains are mutually deformed but the atoms keep their first neighbours (this was rigorously shown by Aubry for the case of the simple chain). The double chain with its connections (springs) has the topology of a structure showing two structural units (figure 2(a)), and which can be produced either by substitution (figure 2(b)), or by hierarchical aggregation (figure 2(c)). These structural units are only a useful construction for this short-range interaction model, and one should not look for them in the real world structure.

The substitution rule illustrated in figure 2(c) produces a unique quasiperiodic composite structure, for which the relative frequency of the two structural units and the ratio of the periods of the two chains is the golden mean ($\tau = \frac{1+\sqrt{5}}{2}$). The hierarchical aggregation is the geometrical representation of relation (19). A hierarchy of periodic structures, whose unit cells have increasing periods and complexity, can be constructed by this method, starting with two given simple basic structures. The relative frequency of the structural units and the ratio of the periods of the two chains can take any rational values, intermediate between the values corresponding to the two basic structures. Also any intermediate quasiperiodic structure can be approximated with arbitrary precision by the periodic structures obtained by hierarchical aggregation. Let us notice the difference between substitution and hierarchical aggregation. While the second method produces a tree of periodic structures, the first method produces only a path of structures inside this tree, leading to a unique quasiperiodic structure, which is the fixed point of the substitution rules. Inside the hierarchical tree, there is an infinite number of such paths, all leading to different quasiperiodic structures which are invariant with respect to different substitution rules of the two structural units.

Finally, we notice that the set $\mathcal{B}$ is a subset of $\mathbb{Z}^2$ contained inside a band, and this property is exactly the same as the one leading to the cut and projection method for generating quasicrystals (Katz and Duneau 1986). If the band is parallel to (p, q) then the composite is (p, q) periodic, if the slope of the band is irrational then the composite is incommensurate. Modifying the width of the band one may modify the range of the interaction (a broader band corresponds to a longer-range interaction).

The part of the dynamical matrix coming from the interchain interaction is:

$$\mathbf{F}'_{p,q}(\theta) = k^{1,2} \left[\begin{array}{c|c} \frac{1}{m_1}\triangle_p^1 & \frac{1}{\sqrt{m_1 m_2}}\mathbf{J}_{p,q} \\ \hline \frac{1}{\sqrt{m_1 m_2}}\mathbf{J}_{p,q}^{\dagger} & \frac{1}{m_2}\triangle_q^2 \end{array}\right]. \tag{20}$$

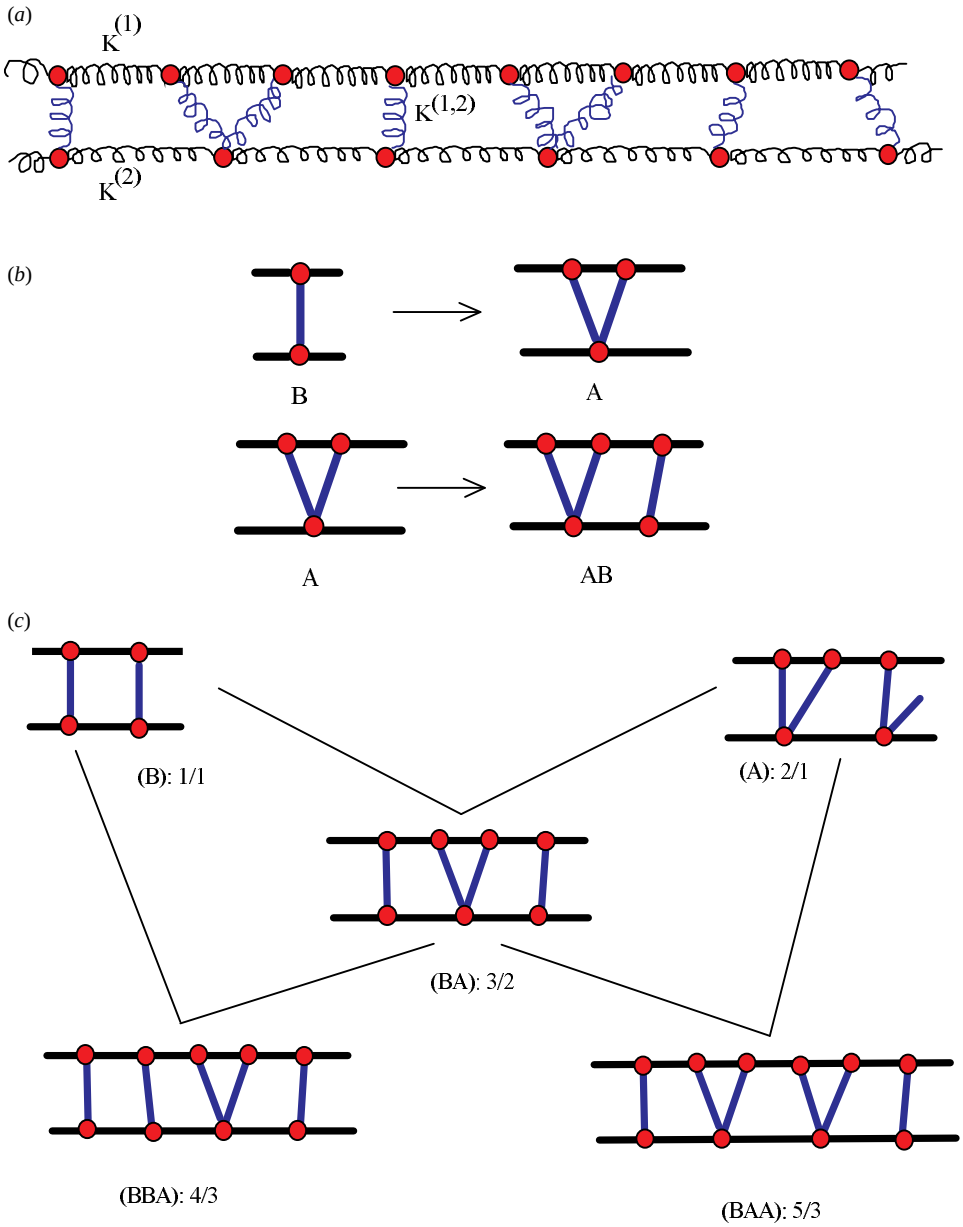

Figure 2. (*a*) Connectivity of a harmonic short-range interaction composite. Larger and larger unit cells may be obtained by (*b*) substitution and (*c*) hierarchical aggregation.

(This figure can be viewed in colour in the electronic version of the article; see `http://www.iop.org/EJ/welcome`)

$\triangle_p^1$ is a p-dimensional diagonal matrix, each diagonal element being $\triangle_p^1(n,n) := \sharp\mathcal{B}_n$ and $\triangle_q^2$ is a q-dimensional diagonal matrix, whose diagonal elements are $\triangle_q^2(m,m) := \sharp\mathcal{B}^m$. For choice (19) one has:

$$\mathrm{Tr}(\triangle_p^1) = \mathrm{Tr}(\triangle_q^2) = p \tag{21}$$

the trace being the number of interchain bonds per unit cell.

The (p, q) matrices $\mathbf{J}_{p,q}$ are obtained by combining (p_1, q_1) and (p_2, q_2) such that $p_1/q_1 < p_2/q_2$:

$$\mathbf{J}_{p_1+p_2,q_1+q_2} = \left[\begin{array}{c|c} \mathbf{J}_{p_1,q_1} & \mathbb{O} \\ \hline \mathbb{O} & \mathbf{J}_{p_2,q_2} \end{array}\right] \qquad \mathbf{J}_{1,1} = [-1] \qquad \mathbf{J}_{2,1} = \begin{bmatrix} -1 \\ -1 \end{bmatrix}. \tag{22}$$

3.2. Hierarchy of gaps in the phonon spectra for even maximum phonon frequency in the two chains ($\omega_1 = \omega_2$)

A formal difficulty in applying perturbation theory to the intercrossing situation comes from the fact that the two values of θ corresponding at fixed $k^{1,2}$, to the minimum and maximum values of the gaps edges are not equal, and they differ from the intercross value of θ. One is forced to apply perturbation theory with variable θ. Precisely, this means solving the eigenvalue problem for the two-dimensional 2D operator $\boldsymbol{F}_{k,l} = \boldsymbol{F}|V_{k,l}(\theta)$, $V_{k,l}(\theta)$ being the space generated by the two intercrossing eigenvectors $v_k^{(1)}(\theta)$ and $v_l^{(2)}(\theta)$. This allows us to find the positions $\lambda_{p,q}^r$ ($r = 1, \ldots, \lfloor \frac{p+q-1}{2} \rfloor$) of the gap centres and the gap widths $\delta\lambda_{p,q}^r$, in first order of $k^{(1,2)}$. Equation (14) has simple solutions only in the case $\omega_1 = \omega_2$, a condition which we suppose to be fulfilled throughout this section. Then, one has (see appendix A):

$$\lambda_{p,q}^r = 4\omega_1^2 \sin^2 \frac{\pi}{p+q} r + \frac{p}{p+q} k^{1,2} \left(\frac{1}{m_1} + \frac{1}{m_2} \right) \tag{23}$$

$$\delta\lambda_{p,q}^r = \frac{k^{1,2}}{\sqrt{m_1 m_2}} \frac{2}{p+q} \frac{p^2+q^2}{pq} \left| P_{p,q}\left[\exp \frac{2\pi \mathrm{i}}{p+q} r \right] \right| \tag{24}$$

$$P_{p_1+p_2,q_1+q_2}(z) = P_{p_1,q_1}(z) + z^{p_1+q_1} P_{p_2,q_2}(z) \qquad \frac{p_1}{q_1} < \frac{p_2}{q_2} \qquad P_{1,1} = 1 \qquad P_{2,1} = 1 + z. \tag{25}$$

The gap widths are exponentially going to zero and their number exponentially increases with n (the order of the approximation), when p/q converges to some irrational value. This is the normal behaviour of approximants of incommensurate structures, of longer and longer periods. The spectrum of the incommensurate limit structure is a Cantor set with infinitely many gaps. For a small perturbation the gap widths are linear in $k^{(1,2)}$, but the perturbation theory applies only for low values of p, q or $k^{(1,2)}$, when the distance between unperturbed levels is much larger than the corresponding matrix elements of the perturbation. For high values of $k^{(1,2)}$, nonlinear effects appear and the aspect of the spectrum changes. We have already seen that when $k^{(1,2)}$ is increased new true gaps may open when single chain gaps superpose, also other gaps may close.

Nevertheless, the '0+' phonon spectrum (infinitesimal small perturbation) for different values of the parameter $\alpha = p/q$, shows remarkable universal features (figure 3), which follow from arithmetic properties of the lattice $\mathbb{Z}^3$. Each gap can be indexed by three integers (p, q, r), and can be embedded in $\mathbb{Z}^3$. The first two integers give the order of the commensurate structure (the ratio of the periods of the two chains). The third integer gives the energetic position of the gap for fixed α. The higher r is, the higher the energy is. Conversely, to each ray (p, q, r) in $\mathbb{Z}^3$, satisfying ($\frac{p+q-1}{2r} \geqslant 1$), there is a gap in the phonon

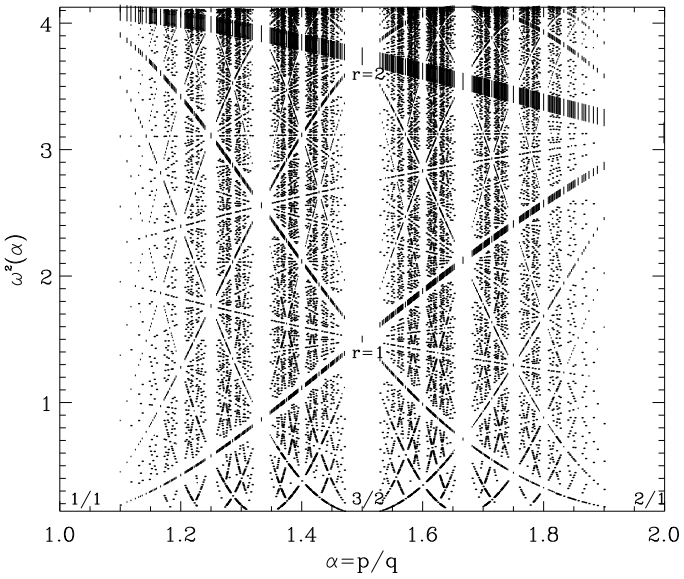

Figure 3. Complementary of the phonon spectra (positions and widths of gaps) for the harmonic short-range interaction composite.

spectrum of the (p, q) periodic composite. The positions of the gaps in the plot $\omega^2(p/q)$ can be obtained from the vertices of $\mathbb{Z}^3$ via a projectivity, followed by two continuous transformations:

$$(p, q, r) \longrightarrow \left(\frac{p}{q}, \frac{r}{q}\right) \longrightarrow \left(\frac{p}{q}, \frac{r}{p+q}\right) \longrightarrow \left(\frac{p}{q}, \lambda^r_{p,q}\right). \tag{26}$$

The above projectivity is the well known gnomonic projection (also called the central projection and used for maps in cartography or for models of the elliptic plane in non-euclidian geometry), and by an elementary theorem of projective geometry, transforms planes into lines and lines into points, as shown in figure 4. This does not say anything about the gap widths, but the interesting affine-projective structure of the gap positions fits nicely to the following generalization of the mediant construction. Two gaps (p_1, q_1, r_1) and (p_2, q_2, r_2) combine to give a third gap $(p_1 + p_2, q_1 + q_2, r_1 + r_2)$, whose width is not very different from the widths of the previous two gaps. The lines occurring in figure 3, along which the gap width seems to depend continuously on α, correspond to 2D sublattices of $\mathbb{Z}^3$ passing through the origin and being generated by (p_1, q_1, r_1) and (p_2, q_2, r_2). These lines can be straightened by a continuous deformation, giving the lines in figure 4. Along such a line the gap widths stay close to a differentiable function $\psi(\alpha)$, going from zero to a maximum value. This maximum value is monotonically non-increasing with the area $\mathcal{S}_2$ of the primitive unit cell of the corresponding 2D sublattice of $\mathbb{Z}^3$. Thus, heavy curves in figure 3 correspond to dense 2D sublattices of $\mathbb{Z}^3$. The fluctuations with respect to $\psi(\alpha)$ are important only for small values of q, for big denominators q, these fluctuations are negligible. For fixed p/q, the fluctuations are monotonically increasing with the value of $\mathcal{S}_2$, and are therefore small for dense 2D sublattices of $\mathbb{Z}^3$ (heavy curves are smoother). A precise statement of these properties, together with detailed proofs will be given elsewhere.

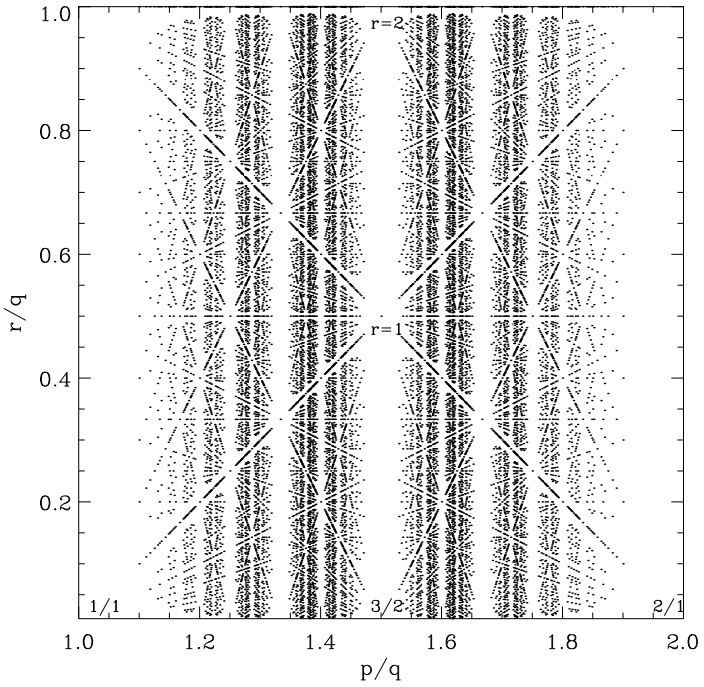

Figure 4. Mapping $\mathbb{Z}^3$ onto the plane by gnomonic projection, transforms planes into lines and lines into points.

3.3. Discontinuity edges in the DOS for arbitrary ω_1, ω_2 and gap hierarchy for $\frac{\omega_1}{\omega_2} \to \infty$

Let us now discuss the situations described by relations (16) and (17). Perturbation theory is simpler in this case, as it can be applied at fixed θ ($\theta = 0, \pm\pi$). Straightforward calculations, along the lines of appendix A, lead to the following results.

(1) The degeneracies $\lambda_k^{(1)}(0) = \lambda_{k'}^{(1)}(0)$ and $\lambda_k^{(1)}(\pm\pi) = \lambda_{k'}^{(1)}(\pm\pi)$ remain also in first order of $k^{(1,2)}$.

(2) Single-chain gaps open in the spectrum of the second chain, linearly in $k^{(1,2)}$. The positions of these single-chain gaps are:

$$\begin{aligned} &\theta = 0 \qquad \lambda_{p,q}^{l}(0) = 4\omega_2^2 \sin^2 \frac{l\pi}{q} + \frac{p}{q}\frac{k^{(1,2)}}{m_2} \\ &l = 1, \ldots, \left\lfloor \frac{q-1}{2} \right\rfloor \\ &\theta = \pi \qquad \lambda_{p,q}^{l}(\pi) = 4\omega_2^2 \sin^2 \frac{\pi}{q}\left(l + \frac{1}{2}\right) + \frac{p}{q}\frac{k^{(1,2)}}{m_2} \\ &l = 1, \ldots, \left\lfloor \frac{q}{2} \right\rfloor \end{aligned} \tag{27}$$

and their widths are:

$$\begin{aligned} &\theta = 0 \qquad \delta\lambda_{p,q}^{l}(0) = \frac{2k^{(1,2)}}{qm_2}\left|Q_{p,q}\left[\exp\left(\frac{2\pi \mathrm{i} l}{q}\right)\right]\right| \\ &\theta = \pi \, \delta\lambda_{p,q}^{l}(\pi) = \frac{2k^{(1,2)}}{qm_2}\left|Q_{p,q}\left[\exp\left(\frac{\pi \mathrm{i}(2l+1)}{q}\right)\right]\right| \end{aligned} \tag{28}$$

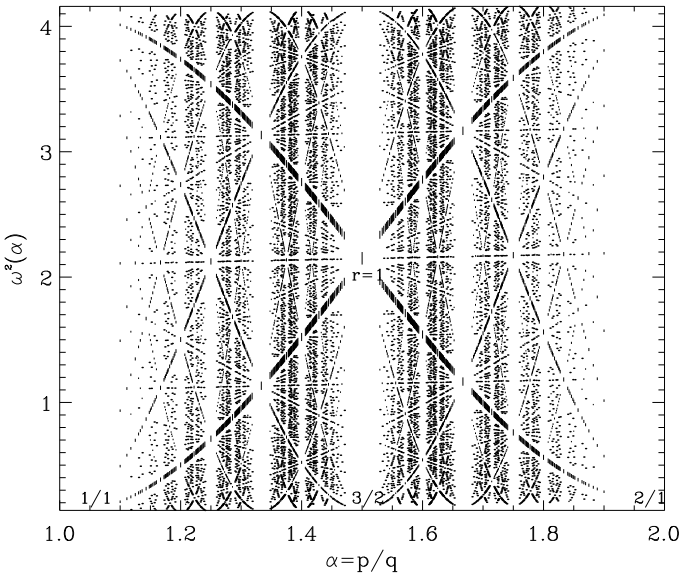

Figure 5. Complementary of the phonon spectra for the Aubry's model (flexible chain on a rigid substrate with parabolic potential).

where the polynomials $Q_{p,q}$ satisfy:

$$\begin{aligned} &Q_{p_1+p_2,q_1+q_2}(w) = Q_{p_1,q_1}(w) + w^{2q_1}Q_{p_2,q_2}(w) \\ &Q_{1,1}(w) = 1 \qquad Q_{2,1}(w) = 2 \end{aligned} \tag{29}$$

for $p_1/q_1 < p_2/q_2$.

Equations (27) and (28) give the positions and the widths of the single chain gaps in the '0+' spectrum of the double chain, but if $\omega_1/\omega_2 \to \infty$ the first chain becomes rigid and the above two equations give the positions and widths of the '0+' spectrum of the Aubry's model (flexible chain on a rigid substrate). The same affine-projective structure as the one discussed in the preceding section also stands in this case, the gap positions obtained from $\mathbb{Z}^3$ by the same projectivity (gnomonic projection), followed by a different continuous transformation. The heavy curves in figure 5 correspond to the same dense 2D sublattices of $\mathbb{Z}^3$ as the heavy curves in figure 3.

4. Sliding mode (phason) and speed of sound

The last type of degeneracy to be discussed is the acoustic degeneracy (15). Before introducing the interchain interaction, there are two zero-energy acoustic phonons of the two chains, each one implying rigid displacement of one chain, while the other chain is fixed:

$$\begin{aligned} &v_0^{(1)}(0) \sim (1, \ldots, 1, 0, \ldots, 0) \\ &v_0^{(2)}(0) \sim (0, \ldots, 0, 1, \ldots, 1). \end{aligned} \tag{30}$$

Let us switch on the interchain interaction in its most general form (2) and solve the secular equation in the 2D space formed by the modes (30). Because F' still has translational

symmetry, there will be a zero-energy acoustic mode:

$$\begin{aligned} v'_{\mathrm{acc}} &\sim (\sqrt{m_1}, \ldots, \sqrt{m_1}, \sqrt{m_2}, \ldots, \sqrt{m_2}) \\ \lambda'_{\mathrm{acc}} &= 0 \end{aligned} \tag{31}$$

and a $k = 0$ phason mode (sliding mode):

$$\begin{aligned} v'_{\mathrm{ph}} &\sim \left(\frac{1}{p\sqrt{m_1}}, \ldots, \frac{1}{p\sqrt{m_1}}, -\frac{1}{q\sqrt{m_2}}, \ldots, -\frac{1}{q\sqrt{m_2}} \right) \\ \lambda'_{\mathrm{ph}} &= k_{\mathrm{eff}}^{(1,2)} \left[\left(1 + \frac{q}{p} \right) \frac{1}{m_1} + \left(1 + \frac{p}{q} \right) \frac{1}{m_2} \right] \\ k_{\mathrm{eff}}^{(1,2)} &= \frac{1}{p+q} \sum_{i \in \mathbb{Z}, j=1,\ldots,q} k_{i,j}^{(1,2)} = \frac{1}{p+q} \sum_{j \in \mathbb{Z}, i=1,\ldots,p} k_{i,j}^{(1,2)}. \end{aligned} \tag{32}$$

The acoustic phonon corresponds to a global rigid displacement of the double chain, while the phason corresponds to relative rigid displacements in opposite directions of the two chains, such that the centre of mass of the double chain remains fixed. Let us recall that the above eigenvectors are in reduced coordinates. In order to obtain the displacements one has to divide the first p coordinates by $\sqrt{m_1}$ and the next q coordinates by $\sqrt{m_2}$.

For the short-range interaction composite discussed in section 3.1, $k_{\mathrm{eff}}^{(1,2)} = k^{(1,2)} \frac{p}{p+q}$ and the phonon gap is finite, even in the incommensurate case. This generalizes the result of Aubry, which shows that the phason is pinned in the case of a flexible chain on a substrate represented by a parabolic potential. It is clear that the only way of depinning it is to allow non-harmonicity of the interchain interaction, i.e. to have an interchain pair potential with both concave and convex parts. In this case, the series defining $k_{\mathrm{eff}}^{(1,2)}$ becomes alternate and may eventually converge to zero, as for the Frenkel–Kontorova model with sinusoidal substrate potential.

Let us now associate a speed of sound to both phonon and phason mode, as follows

$$c = pa \sqrt{\frac{1}{2} \frac{\mathrm{d}^2 \omega^2(\theta)}{\mathrm{d}\theta^2}} \tag{33}$$

where pa is the period of the commensurate double chain. Letting $P_{p,q} = p$ and $k = l = 0$ in (A.9), one obtains in first order of the perturbation:

$$c = \sqrt{\frac{c_1^2 + c_2^2}{2}} \sqrt{1 \pm \frac{c_1^2 - c_2^2}{c_1^2 + c_2^2} \frac{qm_2 - pm_1}{qm_2 + pm_1}} = \sqrt{\frac{c_1^2 + c_2^2}{2}} \sqrt{1 \pm \frac{c_1^2 - c_2^2}{c_1^2 + c_2^2} \frac{\rho_2 - \rho_1}{\rho_2 + \rho_1}} \tag{34}$$

where $c_1 = \omega_1 a, c_2 = \omega_2 b$ are the speeds of sound and ρ_1, ρ_2 are the densities of the decoupled single chains. The positive sign corresponds to the phason, while the negative sign corresponds to the acoustical phonon. If the phason is depinned, then this mode will be detected as a supplementary sound whose speed will be greater or smaller than the phonon speed of sound depending on the sign of $(c_1^2 - c_2^2)(\rho_2 - \rho_1)$.

Finally, we notice that considering the phason displacements to be rigid means that we neglect the intermodulation. If after switching on the interchain interaction the atoms on the two chains move from their regularly distributed positions to the following modulated positions:

$$\begin{aligned} xo_n^{(1)} &= na + \Delta_1 + g^{(1)}(na + \Delta_1) \\ xo_m^{(2)} &= mb + \Delta_2 + g^{(2)}(nb + \Delta_2) \end{aligned} \tag{35}$$

where the phase shifts were chosen to satisfy $\frac{\Delta_1}{\Delta_2} = -\frac{a}{b}\frac{m_2}{m_1}$, and the modulation (or envelope) functions g^i are differentiable, then the following atomic displacements correspond to a zero-energy phason mode (see appendix B):

$$\begin{aligned} u_n^{(1)} &\sim \frac{a}{m_1}[1 + g'^{(1)}(na + \Delta_1)] \\ u_m^{(2)} &\sim \frac{b}{m_2}[1 + g'^{(2)}(mb + \Delta_2)]. \end{aligned} \tag{36}$$

This is consistent with the fact that a pinned phason is always accompanied by a non-differentiable modulation function.

5. Conclusions

Using a double-chain model, we discussed the dynamics of lattice vibrations of a composite structure with two equivalent subsystems. Our results fill a gap in the existing literature on the dynamics of incommensurate structures, where the case of composites is treated only in the hydrodynamic approximation, or using not generally justified descriptions of the interchain interaction.

We show that there are some universal features in the phonon dynamics of composites, common to all incommensurate structures. The energy spectrum of lattice vibrations is a Cantor set for incommensurate composites, and the distribution of gaps for commensurate composites of different periods follows hierarchical rules. Projective geometry is a useful tool for understanding this aspect. The phason mode may or may not be pinned, depending on the form of the interchain potential, as in the case of modulated incommensurate structures.

There are also some specific features that are present in the dynamics of composites. For commensurate double chains the gaps open inside the Brillouin zone, at the intercrossings of phonon branches corresponding to separate chains, when the interchain interaction is switched on. The amplitudon mode is absent, and the phason occurs at the centre of the Brillouin zone. This final property is related to the fact that incommensurability is intrinsic for composites, and it does not appear gradually via a soft mode, as in the case of modulated incommensurate structures. Other specific features of composites are related to static properties of the fundamental states and will be discussed elsewhere.

Although simple, this model may explain dynamical properties of inclusion compounds of the type alcane/urea. The expressions relating the phonon and phason speed of sound to the relative density and rigidity of the subsystems may be directly used for analysing existing available data for light scattering on these compounds (Schmicker *et al* 1995). These experiments seem to prove the existence of an unpinned phason mode having low damping. More complex systems such as $Hg_{3-\delta}AsF_6$ impose extensions of the model. We are presently considering more complicated situations, also involving realistic interaction potentials. The study of eigenvectors and eigenvalues of the dynamical matrix allows the computation of the dynamical structure factor that will be compared with experimental results of neutron diffusion.

Acknowledgments

This work was financed by the CEC grant ERBCHBGCT940690. The authors wish to thank H Cailleau, C Ecolivet, J Etrillard, R Lefort, P van Mouche, J Ollivier, and B Toudic, for inspiring discussions.

Appendix A. Positions and widths of intercrossing gaps for $\omega_1 = \omega_2$

If $\omega_1 = \omega_2$, then the intercross conditions (equations (14) and (13)) lead to

$$\pm\frac{1}{2}\frac{\theta + 2\pi k}{p} = \frac{1}{2}\frac{\theta + 2\pi l}{q} - s\pi \qquad s \in Z. \tag{A.1}$$

It is only the minus sign which is compatible with the condition $\mathrm{d}\lambda_k^{(1)}/\mathrm{d}\theta \mathrm{d}\lambda_l^{(2)}/\mathrm{d}\theta < 0$, necessary for gap opening.

Therefore, the positions of gap openings are

$$\theta_{r'}^{p,q} = \frac{2\pi r'}{p+q} \tag{A.2}$$

with $r' \in \mathbb{Z}$, $-\lfloor p+q-1/2 \rfloor \leqslant r' \leqslant \lfloor p+q-1/2 \rfloor$, and $r' = -(kq+lp)$.

The eigenvalues at the intercrossings are (see equations (13) and (A.2)) :

$$\begin{aligned} &\lambda_k^{(1)}(\theta_{r'}^{p,q}) = \lambda_l^{(2)}(\theta_{r'}^{p,q}) = 4\omega_1^2 \sin^2 \frac{\pi r}{p+q} \\ &r = l - k - \left\lfloor \frac{p+q-1}{2} \right\rfloor \leqslant r \leqslant \left\lfloor \frac{p+q-1}{2} \right\rfloor. \end{aligned} \tag{A.3}$$

The corresponding eigenvectors are given by equation (12), with:

$$z_k = w_l^* = \exp\left[2\pi \mathrm{i}\frac{r}{p+q}\right]. \tag{A.4}$$

The eigenvalues of $F_{k,l}$ are roots of the following second-order equation:

$$\begin{aligned} &\lambda^2 - (\mathrm{Tr}\, F_{k,l})\lambda + \det F_{k,l} = 0 \\ &\mathrm{Tr}\, F_{k,l} = \lambda_k^{(1)}(\theta) + \lambda_l^{(2)}(\theta) + \xi(a_{1,1} + a_{2,2}) \\ &\det F_{k,l} = (\lambda_k^{(1)}(\theta) + \xi a_{1,1})(\lambda_k^{(2)}(\theta) + \xi a_{2,2}) - \xi^2 |a_{1,2}|^2 \end{aligned} \tag{A.5}$$

where

$$\begin{aligned} a_{1,1} &= (v_k^{(1)}(\theta), \mathbf{F}_1^{p,q}(\theta) v_k^{(1)}(\theta)) = \frac{k^{1,2}}{m_1} \\ a_{2,2} &= (v_l^{(2)}(\theta), \mathbf{F}_1^{p,q}(\theta) v_l^{(2)}(\theta)) = \frac{p}{q}\frac{k^{1,2}}{m_2} \\ a_{1,2} &= a_{2,1}^* = (v_l^{(2)}(\theta), \mathbf{F}_1^{p,q}(\theta) v_k^{(1)}(\theta)) = -\frac{k^{1,2}}{\sqrt{m_1 m_2}}\frac{P_{p,q}(z_k^*)}{\sqrt{pq}} \end{aligned} \tag{A.6}$$

and $P_{p,q}(z)$ obeys:

$$\begin{aligned} &P_{p_1+p_2,q_1+q_2}(z) = P_{p_1,q_1}(z) + z^{p_1+q_1} P_{p_2,q_2}(z) \qquad \frac{p_1}{q_1} < \frac{p_2}{q_2} \\ &P_{1,1}(z) = 1 \\ &P_{2,2}(z) = 1 + z. \end{aligned} \tag{A.7}$$

Therefore, the two roots of equation (A.5) are:

$$\begin{aligned} \lambda_{1,2}(\theta) = &\frac{1}{2}[\lambda_k^{(1)}(\theta) + \lambda_l^{(2)}(\theta)] + \frac{1}{2}k^{1,2}\left(\frac{1}{m_1} + \frac{p}{q}\frac{1}{m_2}\right) \\ &\pm\frac{1}{2}\sqrt{\left[\lambda_k^{(1)}(\theta) - \lambda_l^{(2)}(\theta) + k^{1,2}\left(\frac{1}{m_1} - \frac{p}{q}\frac{1}{m_2}\right)\right]^2 + 4\frac{(k^{1,2})^2}{m_1 m_2}\frac{P_{p,q}^2}{pq}}. \end{aligned} \tag{A.8}$$

The extremum condition for the two above eigenvalues branches $\mathrm{d}\lambda_{1,2}(\theta)/\mathrm{d}\theta = 0$ leads to:

$$[\lambda_k^{(1)}(\theta) - \lambda_l^{(2)}(\theta)]^{\pm} = k^{1,2}\left\{-\left(\frac{1}{m_1} - \frac{p}{q}\frac{1}{m_2}\right) \pm \frac{1}{\sqrt{m_1 m_2}}\frac{|P_{p,q}|}{\sqrt{pq}}\frac{|\frac{\mathrm{d}\lambda_k^{(1)}}{\mathrm{d}\theta} + \frac{\mathrm{d}\lambda_l^{(2)}}{\mathrm{d}\theta}|}{\sqrt{-\frac{\mathrm{d}\lambda_k^{(1)}}{\mathrm{d}\theta}\frac{\mathrm{d}\lambda_l^{(2)}}{\mathrm{d}\theta}}}\right\} \tag{A.9}$$

and the positions of the two extrema are, in first order of ξ:

$$\theta^{\pm} = \theta_r^{p,q} + \frac{[\lambda_k^{(1)}(\theta) - \lambda_l^{(2)}(\theta)]^{\pm}}{\frac{\mathrm{d}\lambda_k^{(1)}}{\mathrm{d}\theta} - \frac{\mathrm{d}\lambda_l^{(2)}}{\mathrm{d}\theta}}. \tag{A.10}$$

The values of the derivatives at the intercrossing satisfy:

$$\frac{\frac{\mathrm{d}\lambda_k^{(1)}}{\mathrm{d}\theta}}{\frac{\mathrm{d}\lambda_l^{(2)}}{\mathrm{d}\theta}} = -\frac{q}{p}. \tag{A.11}$$

Introducing (A.9)–(A.11) into (A.8) allows us to find the extreme eigenvalues in the two branches and the gap, as the difference between them:

$$\delta\lambda_{p,q}^{r} = \frac{k^{1,2}}{\sqrt{m_1 m_2}}\frac{2}{p+q}\frac{p^2+q^2}{pq}P_{p,q}\left[\exp\frac{2\pi r\mathrm{i}}{p+q}\right]. \tag{A.12}$$

Appendix B. Acoustic phason for the differentiable modulation function

Here we adapt for the double chain the usual elementary argument employed for the simple Frenkel–Kontorowa model (see Coppersmith and Fisher 1983).

From equation (1) the static equilibrium positions satisfy:

$$\begin{aligned}
&-\mathcal{V}'^{(1,1)}_{n,n+1}(xo^{(1)}_{n+1} - xo^{(1)}_n) + \mathcal{V}'^{(1,1)}_{n-1,n}(xo^{(1)}_n - xo^{(1)}_{n-1}) + \sum_m \mathcal{V}'^{(1,2)}_{n,m}(xo^{(1)}_n - xo^{(2)}_m) = 0\\
&-\mathcal{V}'^{(2,2)}_{m,m+1}(xo^{(2)}_{m+1} - xo^{(2)}_m) + \mathcal{V}'^{(2,2)}_{m-1,m}(xo^{(2)}_m - xo^{(2)}_{m-1}) - \sum_n \mathcal{V}'^{(1,2)}_{n,m}(xo^{(1)}_n - xo^{(2)}_m) = 0.
\end{aligned} \tag{B.1}$$

Introducing the modulated equilibrium positions (35) into (B.1) and then deriving the first equation with respect to Δ_1 and the second equation with respect to Δ_2 one obtains

$$\begin{aligned}
&k^{(1)}\frac{a}{m_1}\{2g'^{(1)}(na+\Delta_1) - g'^{(1)}[(n+1)a+\Delta_1] - g'^{(1)}[(n-1)a+\Delta_1]\}\\
&\qquad + \left(\sum_m k^{(1,2)}_{n,m}\right)\frac{a}{m_1}[g'^{(1)}(na+\Delta_1)+1]\\
&\qquad - \sum_m k^{(1,2)}_{n,m}\frac{b}{m_2}[g'^{(2)}(mb+\Delta_2) - 1] = 0\\
&k^{(2)}\frac{b}{m_2}\{2g'^{(2)}(mb+\Delta_2) - g'^{(2)}[(m+1)b+\Delta_2] - g'^{(2)}[(m-1)b+\Delta_2]\}\\
&\qquad + \left(\sum_n k^{(1,2)}_{n,m}\right)\frac{b}{m_2}[g'^{(2)}(mb+\Delta_2) - 1]\\
&\qquad - \sum_n k^{(1,2)}_{n,m}\frac{a}{m_1}[g'^{(1)}(na+\Delta_1)+1] = 0
\end{aligned} \tag{B.2}$$

which means that displacements (36) belong to the kernel of F (they are zero-energy modes):

$$F\left(\frac{a}{\sqrt{m_1}}[1+g'^{(1)}(na+\Delta_1)], \frac{b}{\sqrt{m_2}}[-1+g'^{(2)}(mb+\Delta_2)]\right) = 0. \tag{B.3}$$

References

Aubry S 1982 Exact models with a complete Devil's staircase *J. Phys. C: Solid State Phys.* **16** 2497–508

Axe J D and Bak P 1982 Long-wavelength excitations in incommensurate intergrowth compounds with application to $Hg_{3-\delta}AsF_6$ *Phys. Rev.* B **26** 4963–73

Coppersmith S N and Fisher D S 1983 Pinning transition of the discrete sine–Gordon equation *Phys. Rev.* B **28** 2566–81

Emery V J and Axe J D 1978 One-dimensional fluctuations and the chain-ordering transformation in $Hg_{3-\delta}AsF_6$ *Phys. Rev. Lett.* **40** 1507–10

Finger W and Rice T M 1983 Long-wavelength phonons in incommensurate systems *Phys. Rev.* B **28** 340–58

Hua L K 1982 *Introduction to Number Theory* (New York: Springer) pp 125–9

Ishii T 1983 Frenkel-Kontorowa model with deformable substrate: ground state and excitation spectrum *J. Phys. Soc. Japan* **52** 168–78

Katz A and Duneau M 1986 *J. Physique* **47** 181–96

de Lange C and Janssen T 1981 Incommensurability and recursivity: Lattice dynamics of modulated crystals *J. Phys. C: Solid State Phys.* **14** 5269–92

van Mouche P 1988 Sur les régions interdites du spectre de l'opérateur périodique et discret de Mathieu *PhD Thesis* Utrecht

Schmicker D, van Smallen S, de Boer J L and Haas C 1995 Observation of the sliding mode in incommensurate intergrowth compound: Brillouin scattering from the inclusion compounds of urea and heptadecane *Phys. Rev. Lett.* **74** 734–7

Theodorou G and Rice T M 1978 Statics and dynamics of incommensurate lattices *Phys. Rev.* B **18** 2840–56

Yamamoto A 1993 Determination of composite crystal structures and superspace groups *Acta Crystallogr.* A **49** 831–46